
Confidence bounds for the true discovery proportion based on the exact distribution of the number of rejections

Friederike Preusse · Anna Vesely · Thorsten Dickhaus

13th October 2023

Abstract In multiple hypotheses testing it has become widely popular to make inference on the true discovery proportion (TDP) of a set \mathcal{M} of null hypotheses. This approach is useful for several application fields, such as neuroimaging and genomics. Several procedures to compute simultaneous lower confidence bounds for the TDP have been suggested in prior literature. Simultaneity allows for post-hoc selection of \mathcal{M} . If sets of interest are specified a priori, it is possible to gain power by removing the simultaneity requirement. We present an approach to compute lower confidence bounds for the TDP if the set of null hypotheses is defined a priori. The proposed method determines the bounds using the exact distribution of the number of rejections based on a step-up multiple testing procedure under independence assumptions. We assess robustness properties of our procedure and apply it to real data from the field of functional magnetic resonance imaging.

Keywords multiple testing · step-up test · cluster inference · false discovery proportion · functional magnetic resonance imaging

F. Preusse
E-mail: preusse@uni-bremen.de
Institute for Statistics, University of Bremen, D-28344 Bremen, Germany

A. Vesely
E-mail: vesely@uni-bremen.de
Institute for Statistics, University of Bremen, D-28344 Bremen, Germany

T. Dickhaus
E-mail: dickhaus@uni-bremen.de
Institute for Statistics, University of Bremen, D-28344 Bremen, Germany

1 Introduction

When testing multiple null hypotheses simultaneously it can be of interest to make inference on sets of null hypotheses instead of on every single null hypothesis. Indeed, inference on each individual null hypothesis with appropriate error control may be very conservative, especially if the number of null hypotheses is large. Moreover, such a fine-grained analysis may not be of particular interest in practical applications. For example, in neuroimaging, brain activation in response to a stimulus is measured at the level of small-scale volume units known as voxels, but the primary interest typically lies in making inference on brain regions that comprise multiple voxels. Similarly, in genomics, inference is often made on collections of genes. In this setting, a global test on a set of null hypotheses only infers whether the set contains at least one false null hypothesis, i.e., at least one true discovery. However, if the set is large, knowing that there is at least one true discovery is unspecific in terms of the total number of true discoveries in the set.

Therefore, in many cases it is of interest to make inference on the number of true discoveries or the corresponding proportion over all the considered null hypotheses (true discovery proportion, TDP). In particular, the computation of lower confidence bounds for the TDP is an active topic of research, (see, e.g., Katsevich & Ramdas 2020; Blain et al. 2022; Andreella et al. 2023; Tian et al. 2023; Vesely et al. 2023). These bounds can be used to answer the following question: If we were to reject all null hypotheses within a set of null hypotheses of interest, how many true discoveries would we find? (Goeman & Solari 2011).

Many procedures that define TDP confidence bounds, including the aforementioned methods, provide them simultaneously for all possible subsets of null hypotheses. This allows the researcher to choose the set of null hypotheses of interest post-hoc, that is, based on the computed confidence bound of the TDP. This is helpful in exploratory research when the sets of null hypotheses of interest have not been defined beforehand. However, the simultaneity requirement potentially reduces power (in a given sense, which we will explain formally in Section 4) and can be removed when the set of interest is known a priori. For instance, in neuroimaging, sometimes researchers may want to explore different brain regions, but in other cases a region of interest is defined a priori (e.g., to test the reproducibility of a study, or to examine whether a region that is known to be associated with a certain stimulus is also associated with a similar one).

In this paper we propose a method to compute lower confidence bounds for the TDP if the subset of interest is specified a priori, assuming that the p-values are independent and their distribution under the alternative is known. The bounds are derived from the exact distribution of the number of rejections of a step-up multiple testing procedure. The proposed method is flexible as any critical vector can be utilized for the step-up procedure. Furthermore, the choice of the critical vector influences the power of the proposed method. Therefore, we derive guidelines on how to select a suitable critical vector. We compare through simulations our proposal to the method of Goeman & Solari (2011), on which most of other proposals in literature are based, demonstrating that we gain power in some settings, especially for low signal strength. Then, we evaluate the robustness of the proposed procedure against violations of the

assumptions, in particular positive dependency between the p-values and misspecification of their distribution under the alternative.

The paper is structured as follows. We review established methods for the computation of lower confidence bounds for the TDP and briefly discuss step-up procedures in Section 2. In Section 3, we introduce the assumptions and our proposed methodology. The choice of the critical vector of the step-up procedure is discussed in Section 4. We compare the performance of the proposed methodology to the procedure by Goeman & Solari (2011) in a simulation study in Section 5 and investigate under which conditions the procedure still yields valid confidence bounds when the model assumptions are violated. In Section 6 we apply the method to a real fMRI data set. We give a brief summary and conclusion in Section 7. Proofs and additional results are given in the Appendix.

2 Background and related literature

In this section we introduce the framework and notation, and briefly discuss related work. First we consider methods to make inference on the TDP, reviewing existing literature; subsequently we introduce step-up tests on which our proposed method will rely.

2.1 Inference on the TDP

Let $\mathcal{M} = \{H_1, \dots, H_m\}$ be a non-empty collection of null hypotheses and denote by $\mathcal{M}_1 \subseteq \mathcal{M}$ the unknown subset of false null hypotheses (true discoveries). We are interested in making inference on the number of true discoveries $m_1 = |\mathcal{M}_1|$, where $|\cdot|$ denotes the size of a set, or equivalently the proportion of true discoveries $\pi_1 = m_1/m$. In fMRI data analysis, for instance, \mathcal{M} may correspond to a region of the brain having m voxels, while m_1 and π_1 are the number and the proportion of truly active voxels (which equals the TDP in that context), respectively.

For any $\alpha \in (0, 1)$, we will compute a lower $(1 - \alpha)$ -confidence bound for the number of true discoveries, i.e., a value \hat{m}_1 such that

$$\mathbb{P}(m_1 \geq \hat{m}_1) \geq 1 - \alpha, \quad (1)$$

where \mathbb{P} refers to the probability measure under the true but unknown data generating process. From \hat{m}_1 we can immediately derive confidence bounds for other quantities of interest such as the TDP and the number or proportion of false discoveries (Goeman & Solari 2011). For instance, a lower confidence bound for the TDP is $\hat{\pi}_1 = \hat{m}_1/m$, while an upper confidence bound for the number of false discoveries is $\hat{m}_0 = m - \hat{m}_1$.

Many procedures have been proposed that focus on simultaneous inference on the TDP based on confidence bounds (Genovese & Wasserman 2006; Meinshausen 2006; Goeman & Solari 2011; Lee et al. 2012; Rosenblatt et al. 2018; Hemerik et al. 2019; Blanchard et al. 2020; Ebrahimpour et al. 2020; Blain et al. 2022; Cai et al. 2022; Andreella et al. 2023; Vesely et al. 2023). Such procedures make inference on

the TDP simultaneously over all possible subsets of hypotheses. In this case, the set \mathcal{M} is allowed to vary as any subset of a bigger multiple testing problem. For example, in fMRI data, different brain regions can be analyzed simultaneously. This allows for post-hoc inference, as the confidence bounds are valid even if we select the subset of interest after computing the bounds. Goeman & Solari (2011) emphasize this exploratory aspect of simultaneous TDP confidence bounds and show that simultaneity of the bounds is assured by embedding any global test into the closed testing framework (Marcus et al. 1976). It has been shown that this approach is equivalent to an earlier proposal by Genovese & Wasserman (2006) (Goeman, Hemerik, & Solari 2021) and, if permutation tests are used, these bounds are identical to those proposed in Meinshausen (2006) (Goeman & Solari 2011). First applications of the method to fMRI data (Rosenblatt et al. 2018) and to genomics data (Ebrahimipour et al. 2020) rely on the comparison between a vector of ordered p-values and the critical vector based on the Simes test (Simes 1986). A more flexible variant of the method is proposed in Hemerik et al. (2019) and Andreella et al. (2023), who use conditional resampling to define a critical vector. To do so, families of critical vectors, i.e., collections of critical vectors based on the same critical value function, are defined a priori. Randomization is used to define the critical vector from the family, such that the chosen critical vector provides the highest valid confidence bound for the TDP. Similar procedures are proposed by Blanchard et al. (2020) and Blain et al. (2022). The latter extends the method by constructing the families of critical vectors using additional randomization. Simultaneous inference on the TDP is an active topic of research, further developments can be found in Katsevich & Ramdas (2020), Davenport et al. (2022), X. Chen et al. (2023), Tian et al. (2023) and Goeman et al. (2023).

If the set of null hypotheses \mathcal{M} that we want to make inference on is selected a priori, we can potentially gain power by removing the simultaneity requirement. Such a confidence bound for the TDP has been proposed in Patra & Sen (2016) for the two-groups mixture model of the p-values, as defined by Efron et al. (2001). Our proposed method assumes a conditional version of the two-group mixture model, in accordance with Roquain & Villers (2011). Similarly to Hemerik et al. (2019), Andreella et al. (2023) and Blanchard et al. (2020), our procedure relies on a critical vector chosen from an a priori defined family of critical vectors. Contrarily to their methods, all critical vectors in the family provide valid confidence bounds, so we can choose the critical vector that provides the highest bound possible. We assume that the distribution of the p-values is known, but demonstrate through simulations that the method is robust to certain misspecifications of their distribution.

2.2 Step-up procedures

In this section we will give a short introduction to step-up tests. We first define the properties of such a procedure and then present some established tests. An exhaustive introduction to the topic is given in Dickhaus (2014), Chapter 5.

Multiple testing procedures are defined as functions that return a set of rejected null hypotheses based on the observed p-values. Formally, let P_1, \dots, P_m be random p-values for the null hypotheses of interest, and let p_1, \dots, p_m be their observed val-

ues. A multiple testing procedure rejects a subset $\mathcal{R} \subseteq \mathcal{M}$ of null hypotheses. A step-up test is a particular multiple testing procedure that determines \mathcal{R} by sorting the observed p-values and comparing them to a critical vector with the following properties.

Definition 1 A vector $(t_1, \dots, t_m)^\top \in [0, 1]^m$ is a critical vector for a step-up procedure if it is non-decreasing: $0 \leq t_1 \leq \dots \leq t_m \leq 1$.

Given a critical vector, the step-up procedure is defined as follows.

Definition 2 Denote by $(p_{1:m}, \dots, p_{m:m})^\top \in [0, 1]^m$ the vector of ordered observed p-values, so that $p_{1:m} \leq \dots \leq p_{m:m}$. Let $H_{1:m}, \dots, H_{m:m}$ be the corresponding ordered null hypotheses. Then let $k = \max\{i = 1, \dots, m \mid p_{i:m} \leq t_i\}$. A step-up procedure rejects $\mathcal{R} = \{H_{1:m}, \dots, H_{k:m}\}$ if k exists, and $\mathcal{R} = \emptyset$ otherwise.

Step-up tests can be constructed to control the family-wise error rate (FWER), the false discovery rate (FDR), or other error measures. Critical vectors change based on the desired error rate control level. While our method makes use of a generic step-up test, without requiring control of the FWER or FDR, we use the structure of established tests (i.e., established families of critical vectors) to derive critical vectors. In particular, we will focus on critical vectors defined for FDR control. The most famous procedure is the linear step-up test by Benjamini & Hochberg (1995), which is based on the critical value function by Simes (1986). The power of the test can be improved by including additional information in the procedure, such as an estimate for the number of true null hypotheses (Benjamini & Hochberg 2000; Sarkar 2002; Storey et al. 2004; Hwang 2011, for an overview and comparison). Finner et al. (2009) studied the asymptotic behavior of step-up-down tests (i.e., $m \rightarrow \infty$) and proposed an asymptotically optimal rejection curve (AORC), with optimality in the sense of optimal power. Critical value functions based on the AORC are given in Finner et al. (2009), Gontcharuk (2010), Finner et al. (2012) and Habiger & Adekpedjou (2014). For arbitrary dependency among the p-values, Benjamini & Yekutieli (2001) adapted the procedure by Benjamini & Hochberg (1995), while a new family of step-up tests is proposed in Blanchard & Roquain (2008).

Properties of step-up tests are investigated in Finner & Roters (2002), Cohen & Sackrowitz (2007), Ferreira & Zwinderman (2006), Roquain & Villers (2011) and J. Chen et al. (2011), among others. Under the assumption that all null hypotheses are true, Finner & Roters (2002) derived the exact distribution of the number of rejected hypotheses for step-up procedures. The exact distribution of the false discovery proportion for step-up and step-down tests for different p-value models is given in Roquain & Villers (2011). Explicit formulas for different notions of power for step-wise procedures are given in J. Chen et al. (2011). Scenarios in which step-up tests cannot be employed are described in Cohen & Sackrowitz (2007).

3 Methodology

In this section we propose a procedure to obtain a lower confidence bound for the number m_1 of true discoveries, denoted by \hat{m}_1 as in Eq. (1). We assume that the p-value follow the model referred to as “unconditional independent model” by Roquain

& Villers (2011), so that the stochastically independent p-values corresponding to false null hypotheses follow the same cumulative distribution function (CDF) F .

Assumption 1 *The p-values P_1, \dots, P_m are stochastically independent and have the following (marginal) distribution:*

$$P_i \sim \begin{cases} F & \text{if } 1 \leq i \leq m_1 \\ \text{Uni}[0, 1] & \text{if } m_1 + 1 \leq i \leq m. \end{cases}$$

While F is assumed to be known, the number of true discoveries m_1 is not. We denote by \mathbb{P}_{m_1} the probability measure under this model and compute the desired confidence bound in Eq. (1) under this probability measure. For simplicity of notation, we notationally omit dependency on m and F , as well as any other fixed quantities defined throughout the paper.

As mentioned in the previous section, we rely on a step-up procedure. Hence consider a step-up procedure, as given in Definition 2, that uses a pre-fixed critical vector $(t_1, \dots, t_m)^\top$ and rejects a subset \mathcal{R} of hypotheses. Denote by $R = |\mathcal{R}|$ the random variable representing the number of rejections and denote by r its observed value. Note that R is a function of the p-values that takes values in $\{0, \dots, m\}$.

Fix any $\alpha \in (0, 1)$. The following theorem shows how to compute the desired lower $(1 - \alpha)$ -confidence bound \hat{m}_1 , following from Remark 2 in von Schroeder & Dickhaus (2020). Throughout the paper, we denote by $\tilde{m}_1 \in \{0, \dots, m\}$ a generic candidate for the number of true discoveries, and by $\mathbb{P}_{\tilde{m}_1}$ the probability measure under the same model of Assumption 1, but having \tilde{m}_1 false null hypotheses instead of m_1 .

Theorem 1 *For any $\tilde{m}_1 \in \{0, \dots, m\}$, let*

$$\gamma_{\tilde{m}_1} = \max\{\gamma \in [0, 1] \mid \mathbb{P}_{\tilde{m}_1}(\tilde{m}_1 \geq R\gamma) \geq 1 - \alpha\}. \quad (2)$$

Subsequently, define

$$\hat{m}_1 = \lceil r\gamma^* \rceil \quad \text{as well as} \quad \gamma^* = \min_{\tilde{m}_1 \in \{0, \dots, m\}} \gamma_{\tilde{m}_1}, \quad (3)$$

where $\lceil \cdot \rceil$ represents the ceiling function. Then

$$\mathbb{P}_{m_1}(m_1 \geq \hat{m}_1) \geq 1 - \alpha. \quad (4)$$

A formal proof is provided in Appendix A. The main idea is to consider each possible value \tilde{m}_1 for the number of true discoveries, ranging from 0 to m . Under the corresponding model and probability measure $\mathbb{P}_{\tilde{m}_1}$, we determine $\gamma_{\tilde{m}_1}$ as the largest value such that $\mathbb{P}_{\tilde{m}_1}(\tilde{m}_1 \geq R\gamma_{\tilde{m}_1}) \geq 1 - \alpha$. Notice that here all quantities are fixed, with the exception of the random variable R . Subsequently, we take γ^* as the minimum of all values $\gamma_{\tilde{m}_1}$. It follows immediately that $\mathbb{P}_{\tilde{m}_1}(\tilde{m}_1 \geq R\gamma^*) \geq 1 - \alpha$ for any \tilde{m}_1 , and in particular this holds for the true, unknown value m_1 . Finally, the use of the ceiling function follows from the fact that m_1 can take only integer values.

From \hat{m}_1 we can immediately derive a confidence bound for the TDP by using $\hat{\pi}_1 = \hat{m}_1/m$. We underline that the number of true discoveries and the TDP are defined

considering the entire set \mathcal{M} of hypotheses, and not with respect to the subset \mathcal{R} of hypotheses that are rejected by the step-up procedure. Indeed, the step-up procedure is used only as a tool to construct the desired confidence bound, but the procedure does not require to associate any error control with \mathcal{R} . In the next sections we will show how to compute the confidence bound \hat{m}_1 in practice.

3.1 Computation of the lower confidence bound

To compute γ^* and thus the desired confidence bound \hat{m}_1 we need to determine $\gamma_{\tilde{m}_1}$ as in Eq. (2) for all possible values of \tilde{m}_1 and then to evaluate the minimum.

Fix any $\tilde{m}_1 \in \{0, \dots, m\}$. Eq. (2) requires to explore all values $\gamma \in [0, 1]$. The following theorem shows that $\gamma_{\tilde{m}_1}$ can be computed using the distribution of the number of rejections R under $\mathbb{P}_{\tilde{m}_1}$.

Theorem 2 For $\tilde{m}_1 = 0$,

$$\gamma_0 = \begin{cases} 1 & \text{if } \mathbb{P}_{\tilde{m}_1}(R = 0) \geq 1 - \alpha \\ 0 & \text{otherwise.} \end{cases}$$

For $\tilde{m}_1 \in \{1, \dots, m\}$, $\gamma_{\tilde{m}_1} = \tilde{m}_1 / \ell_{\tilde{m}_1}$, where

$$\ell_{\tilde{m}_1} = \min \{ \ell \in \{ \tilde{m}_1, \dots, m-1, m \} : \mathbb{P}_{\tilde{m}_1}(R \leq \ell) \geq 1 - \alpha \}.$$

As R is a discrete variable, Theorem 2 shows that $\gamma_{\tilde{m}_1}$ can be computed evaluating the probability distribution of R on a finite number of points, namely one if $\tilde{m}_1 = 0$ and $m - \tilde{m}_1$ otherwise. Furthermore, note that $\gamma_{\tilde{m}_1}$ and therefore γ^* do not depend on observations and do not change as long as the distribution of R does not change. This allows us to compute γ^* as soon as F is known, before seeing the data, since R is a function of the p-values. The observed data in form of the observed number of rejected hypotheses r are only used when computing \hat{m}_1 from Eq. (3).

In the next section we give the distribution of R for step-up tests.

3.2 Distribution of the number of rejections R

Equations given in Roquain & Villers (2011), Section 5.3, can be used to compute the distribution of the number of rejections R . As in the previous sections, consider a generic step-up test that relies on a critical vector $(t_1, \dots, t_m)^\top$. The following proposition gives the distribution of the random number R of rejections of this step-up test.

Proposition 1 Fix any $\tilde{m}_1 \in \{0, \dots, m\}$ and the probability measure $\mathbb{P}_{\tilde{m}_1}$ under the corresponding model. Then, for any $\ell \in \{0, \dots, m\}$,

$$\begin{aligned} \mathbb{P}_{\tilde{m}_1}(R \leq \ell) &= \sum_{k=0}^{\ell} \sum_{j=0}^k \binom{m - \tilde{m}_1}{j} \binom{\tilde{m}_1}{k-j} t_k^j (F(t_k))^{k-j} \\ &\quad \cdot \Psi_{m - \tilde{m}_1 - j, \tilde{m}_1 - k + j}^{Uni[0,1], \bar{F}}(1 - t_m, \dots, 1 - t_{k+1}), \end{aligned}$$

where $\bar{F}(t) = 1 - F(1 - t)$ and $\Psi_{m-\tilde{m}_1-j, \tilde{m}_1-k+j}^{Uni[0,1], \bar{F}}$ denotes the joint distribution of $m - k$ ordered independent random variables, where $m - \tilde{m}_1 - j$ follow the uniform distribution $Uni[0, 1]$ and the remaining ones have CDF F . This relates to the joint distribution of the ordered p -values that correspond to hypotheses not rejected by the underlying step-up procedure.

The joint distribution of order statistics can be computed using generalized recursions as given in von Schroeder & Dickhaus (2020).

In summary, the lower $(1 - \alpha)$ -confidence bound \hat{m}_1 for the number of true discoveries given in Theorem 1 is computed considering all possible values $\tilde{m}_1 \in [0, m]$, evaluating for each of them the maximum of a given function defined from the distribution of the random number of rejections R of a step-up test. This maximum can be determined by computing the distribution of R for a finite number of points. The algorithm to compute \hat{m}_1 is given in Appendix B.

4 Choice of the critical vector

Any choice of the critical vector of the step-up procedure that satisfies Definition 1 leads to a valid confidence bound \hat{m}_1 ; however, this choice influences the procedure's performance. In this section, we present some of the families of critical vectors discussed in Section 2 as well as a new one, then we illustrate how to select a suitable critical vector from a family which is assumed to be fixed a priori. Suggestions on the choice of the family of critical vectors are given in Section 5.

A family of critical vectors can be defined as a collection of curves depending on one or more parameters. A particular critical vector $(t_1, \dots, t_m)^\top$ can be chosen from the family by fixing the parameter values. A first example is the family of linear critical vectors proposed by Benjamini & Hochberg (1995), defined by

$$t_i(\lambda) = \frac{i}{m} \lambda, \quad \lambda \in [0, 1]. \quad (5)$$

We denote this family by “*BH*”. Another linear approach is that of Benjamini & Yekutieli (2001):

$$t_i(\lambda) = \frac{i/m \cdot \lambda}{\sum_{j=1}^m \frac{1}{j}}, \quad \lambda \in \left[0, \sum_{j=1}^m \frac{1}{j}\right] \quad (6)$$

which we denote by “*BY*”. Critical vectors based on the AORC can also be employed. One possible family is given by Finner et al. (2009):

$$t_i(\lambda, \beta) = \frac{i \cdot \lambda}{m + \beta - i \cdot (1 - \lambda)}, \quad \lambda \geq 0, \quad \beta \geq 0. \quad (7)$$

This family is denoted by “*AORC*”. Note that λ could also be negative, then $\beta < -m$, however, we focus on $\lambda \leq 0$ due to its original interpretation as the level of FDR control in Finner et al. (2009). Furthermore, we consider a new family which has a more flexible shape than *AORC*, *BH* and *BY*:

$$t_i(\lambda, \beta) = \lambda \cdot \left(\frac{i}{m}\right)^\beta, \quad 0 \leq \lambda \leq 1, \quad \beta \geq 0. \quad (8)$$

Depending on β it is either a convex function ($\beta > 1$), or a concave function ($\beta < 1$), or a linear function ($\beta = 1$). This procedure is denoted by “Exp”.

Note that the choice of the parameters, and consequently of the critical vector used in the procedure, is up to the practitioner. However, it is desirable that the procedure has high power and low variability, i.e., that the resulting confidence bound has a high expected value $E_{m_1}[\hat{m}_1]$ and low variance $Var_{m_1}[\hat{m}_1]$ under the true data generating model. In the following paragraphs we illustrate how to select the parameters in order to meet these requirements.

Fix any critical vector $(t_1, \dots, t_m)^\top$, for which the corresponding step-up procedure rejects R hypotheses. Recall that $\hat{m}_1 = \lceil r\gamma^* \rceil$ depends on the realization of the random variable R and on γ^* , which in turn depends on the distribution of R . Since such distribution is known, it is possible to determine the expected value and variance of \hat{m}_1 with respect to any probability measure $\mathbb{P}_{\tilde{m}_1}$. However, these values cannot be computed in closed form due to the ceiling function appearing in Eq. (3); for this reason, we consider $r\gamma^* \approx \hat{m}_1$ instead.

Proposition 2 Fix any $\tilde{m}_1 \in \{0, \dots, m\}$ and the probability measure $\mathbb{P}_{\tilde{m}_1}$ under the corresponding model. Then

$$\begin{aligned} E_{\tilde{m}_1}[R\gamma^*] &= \gamma^* \cdot E_{\tilde{m}_1}[R] \\ &= \gamma^* \cdot \sum_{\ell=0}^m \ell \cdot \left(\sum_{j=0}^{\ell} \binom{m-\tilde{m}_1}{j} \binom{\tilde{m}_1}{\ell-j} (t_\ell)^j (F(t_\ell))^{\ell-j} \right. \\ &\quad \left. \cdot \Psi_{m-\tilde{m}_1-j, \tilde{m}_1-\ell+j}^{Uni[0,1], F}(1-t_m, \dots, 1-t_{\ell+1}) \right). \end{aligned}$$

Furthermore,

$$Var_{\tilde{m}_1}[R\gamma^*] = (\gamma^*)^2 \cdot Var_{\tilde{m}_1}[R]$$

with

$$\begin{aligned} Var_{\tilde{m}_1}[R] &= \sum_{\ell=0}^m \ell^2 \cdot \left[\sum_{j=0}^{\ell} \binom{m-\tilde{m}_1}{j} \binom{\tilde{m}_1}{\ell-j} (t_\ell)^j F(t_\ell)^{\ell-j} \right. \\ &\quad \left. \cdot \Psi_{m-\tilde{m}_1-j, \tilde{m}_1-\ell+j}^{Uni[0,1], \bar{F}}(1-t_m, \dots, 1-t_{\ell+1}) \right] \\ &\quad - \left(\sum_{\ell=0}^m \ell \cdot \left[\sum_{j=0}^{\ell} \binom{m-\tilde{m}_1}{j} \binom{\tilde{m}_1}{\ell-j} (t_\ell)^j F(t_\ell)^{\ell-j} \right. \right. \\ &\quad \left. \left. \cdot \Psi_{m-\tilde{m}_1-j, \tilde{m}_1-\ell+j}^{Uni[0,1], \bar{F}}(1-t_m, \dots, 1-t_{\ell+1}) \right] \right)^2. \end{aligned}$$

As previously mentioned, $E_{m_1}[R\gamma^*]$ is desired to be as high as possible. As the real value of m_1 is not known, we require that the expected value is as high as possible over all possible values of \tilde{m}_1 , considering

$$\sum_{\tilde{m}_1=0}^m E_{\tilde{m}_1}[R\gamma^*]. \quad (9)$$

For any pre-fixed family of critical vectors, we suggest computing this sum for different choices of the parameters and selecting the one that maximizes it. For the

considered families of critical vectors and normally distributed data, simulations indicate that Eq. (9) is maximized when using the critical vector with the largest λ for which $\gamma^* = 1$. This holds true for families of critical vectors with two parameters as well. Furthermore, the simulations indicate that the choice of maximizing Eq. (9) is reasonable, as the optimal critical vector determined in this way maximizes also $E_{m_1}[R\gamma^*]$ in most settings. These simulation results are displayed in Appendix C.

If different parameter combinations for families with two parameters have similar power, we can use the one having the smallest variance. Analogously to the case of the expected value, we consider the sum

$$\sum_{\tilde{m}_1=0}^m \text{Var}_{\tilde{m}_1}[R\gamma^*]. \quad (10)$$

Then the procedure to obtain critical vectors from a family with two parameters is the following. For varying values of β , find, using a grid search algorithm, the respective value of λ such that Eq. (9) is maximized. Then select the parameter combinations for which Eq. (9) is the maximum or reasonably close to it. Finally, among these combinations, select the one that minimizes Eq. (10).

To summarize, when choosing the critical vector, achieving high power is the main priority. For families of critical vectors with more than one parameter, different combinations may lead to the same, or similar, power. In this case, the parameter combination minimizing the variance should be chosen. As we will illustrate in the following section, in practical applications it can be sensible to sacrifice some power to reduce the variance, as it might increase the robustness of our methodology to violations of the model assumptions.

5 Simulations

In this section we discuss simulation results. We have compared the performance of our procedure with the procedure by Goeman & Solari (2011). We have focused on this comparison, as other approaches mentioned in Section 2 are either derived from it or based on permutations and therefore defined in a different framework. First, we have studied the methods under Assumption 1, i.e., independence of the p-values and the correct specification of the CDF F . Subsequently, we have investigated the robustness of our procedure to violations of these assumptions. Finally we have explored different approaches to estimate the parameters of F .

We have simulated N stochastically independent and identically distributed (i.i.d.) observables X_1, \dots, X_N from a m -variate equicorrelated multivariate normal distribution with all marginal variances equal to one and correlation coefficient ρ , such that the stochastic representation $X_1 = \eta + \varepsilon \in \mathbb{R}^m$ with $\varepsilon \sim \text{MVN}_m(\mathbf{0}, \Sigma_\rho)$ holds true, where $\text{MVN}_m(\mathbf{0}, \Sigma_\rho)$ denotes the m -variate normal distribution described before. The entries of the vector η are equal to η_{alt} for the first m_1 entries and zero for the remaining ones. We have varied η_{alt} to account for different effect sizes θ , where $\eta_{alt} = \theta/\sqrt{2}$. While the assumption of (approximately) normally distributed data is often justified in practice, often only (some) information about the effect size

is available. With this, we mean that the practitioner typically neither knows the marginal variances of X_1 nor that these marginal variances are all equal to each other. This necessitates Studentizing all m coordinates of X_1, \dots, X_N separately in a practical data analysis situation, which we emulate here. Furthermore, we underline that the normal distribution model is the standard model used in fMRI analysis to detect activation (Lindquist 2008). For each variable we have tested the null hypothesis that the mean is zero against a two-sided alternative and we have obtained a t-statistic and the corresponding p-value via a two-sided one-sample t-test. If a null hypothesis H_i is false, the t-statistic is $Q_i \sim F_{v,\mu}$, where $F_{v,\mu}$ denotes the CDF of the t-distribution with non-centrality parameter $\mu = \theta \cdot \sqrt{N/2} = \eta_{alt} \cdot \sqrt{N}$ and $v = N - 1$ degrees of freedom. The corresponding p-value is $P_i \sim F$, where

$$F(p) := 1 - F_{v,0} \left(F_{v,\mu}^{-1} \left(1 - \frac{p}{2} \right) \right) + F_{v,0} \left(-F_{v,\mu}^{-1} \left(1 - \frac{p}{2} \right) \right). \quad (11)$$

Subsequently, we have applied the procedure by Goeman & Solari (2011) (“*GS*”) and the proposed method to compute a lower $(1 - \alpha)$ -confidence bound \hat{m}_1 for the number of true discoveries. For the latter, we have considered different critical vectors, chosen from the families introduced in Section 4: *BH* (Eq. (5)), *BY* (Eq. (6)), *AORC* (Eq. (7)) and *Exp* (Eq. (8)). Throughout the following sections, we use the same notation to identify a family and results obtained using the family within our procedure, leaving distinction to context.

For each family, parameters were selected so that the critical vector maximizes Eq. (9) (denoted by suffix “opt”), which in this setting always corresponds to the largest value of the parameter λ such that $\gamma^* = 1$. To further investigate the behavior of the method, when possible we have studied additional critical vectors, taking the largest λ such that $\gamma^* = 0.95$ (denoted by suffix “0.95”), $\gamma^* = 0.9$ (“0.9”) and $\gamma^* = 0.8$ (“0.8”). Families with two parameters for which different parameter combinations could lead to the same value γ^* have been managed as suggested in the previous section. The performance of our methodology with different critical vectors as well as the performance of the *GS* procedure have been studied. First, we have examined the validity of the confidence bounds, that is, checking that the proportion of iterations for which $m_1 < \hat{m}_1$ is at most α . Then we have compared results in terms of power and variability, i.e., the average and the empirical variance of the computed confidence bounds over all iterations.

All results are based on $N = 50$ observations, $m = 100$ hypotheses and significance level $\alpha = 0.2$. We have set the number of true discoveries as $m_1 \in \{5, 10, 20, 30, \dots, 90\}$. First, we have simulated the data and applied the procedure under the assumptions of the model, fixing the correlation parameter $\rho = 0$ and assuming that the true effect size θ , and thus F , are known. We have considered $\theta \in \{0.4, 0.6, 0.8, 1, 1.2, 2, 5\}$, as well as $\theta = -1$ to check whether negative effect sizes lead to different results. Subsequently, we have analyzed the robustness of the method to violations of the independence assumption or misspecification of F . For the first case, we have varied the correlation parameter ρ . Note that X_1, \dots, X_N remain i.i.d. under any value of ρ . For the second case, we have used a value $\hat{\theta}$ instead of the true effect size θ in the procedure. In practice, $\hat{\theta}$ can be an estimate determined using prior information

or by estimating the effect size from external data from the same experiment or a similar one. Each scenario has been simulated $B = 10,000$ times.

All simulations were carried out in R (R Core Team 2022). We have used the `homme1` package (Goeman, Meijer, & Krebs 2021) for *GS*, as well as the `OrdStat` package, available at github.com/jvschroeder/OrdStat, to compute the joint distribution of order statistics as in von Schroeder (2018). The code for the proposed method is available upon request to the authors.

The following sections show results for each scenario, while additional results and figures are reported in Appendix C. Since using the negative effect size $\theta = -1$ leads to similar results as the corresponding positive effect size $\theta = 1$, results for $\theta = -1$ are not stated explicitly. Furthermore, *BH* and *BY* generally lead to similar results, therefore only results based on *BH* are reported. Finally, for the smallest effect size ($\theta = 0.4$), it was not possible to find critical vectors such that $0 < \gamma^* < 1$ for families with one parameter, so only results for $\gamma^* = 1$ have been considered.

5.1 Independence

First we show results under the assumptions of the model, i.e., for independent p-values ($\rho = 0$) and correct specification of the distribution F . These are discussed in terms of the resulting lower confidence bound \hat{m}_1 : validity, power and variability.

As expected, all methods determine valid confidence bounds. Power tends to increase with the value of γ^* used to choose the critical vector, confirming what has been stated in Section 4. Hence, for each family the highest power is achieved choosing the critical vector so that $\gamma^* = 1$. Moreover, for all procedures power increases with the effect size θ .

Figure 1 displays the average confidence bounds \hat{m}_1 obtained from *GS* and the proposed method with different families and using $\gamma^* = 1$. Results are shown for the smaller effect sizes ($\theta \leq 1.2$) and the extreme values of the denseness of signal ($m_1 \in \{10, 90\}$). For small effect sizes ($\theta \leq 1$), the proposed method using any family and $\gamma^* = 1$ is more powerful than *GS*. In particular, the highest power is achieved with *Exp_{opt}* when the signal is sparse (low m_1), and with *AORC_{opt}* when it is dense (large m_1). *BH_{opt}* is generally the second most powerful procedure. On the contrary, for large effect sizes *GS* is generally the most powerful procedure, followed by *BH_{opt}* and *AORC_{opt}*.

For all methods, the empirical variance increases as θ decreases, with a slower increase for *GS*. For small θ , *GS* has the lowest empirical variance; for the proposed procedure, the empirical variance decreases with γ^* . The opposite is true for large θ : the empirical variance is higher for *GS*, and in the proposed method decreases as γ^* increases. This indicates that there is not a linear relationship between the empirical variance and γ^* .

5.2 Dependency among the p-values

To investigate the robustness of our procedure to the violation of the independence assumption we have set the level of correlation $\rho \in \{0.3, 0.6, 0.9\}$, while F is still

correctly specified. Note that we have only used positive correlation coefficients because in applications such as fMRI data positive dependency of the voxels is assumed (Lindquist 2008).

For larger effect sizes ($\theta \geq 1$), all methods determine valid confidence bounds for any level of correlation, except *Exp* with $\gamma^* < 1$ for large effect size ($\theta \geq 2$). As the effect size decreases, the proposed method determines valid confidence bounds using any family with decreasing γ^* . Regarding power, for larger effect sizes ($\theta \geq 2$) it increases with ρ ; in this setting, *GS* remains the most powerful method. For smaller effect sizes ($\theta \leq 0.8$), the proposed method using any family with the largest γ^* that leads to valid confidence bounds is more powerful than *GS*. The empirical variance of all methods increases with the level of correlation ρ . For larger effect sizes ($\theta \geq 1.2$) this increase is faster for *GS*. Otherwise, results concerning the empirical variance are similar to the independent case ($\rho = 0$).

5.3 Misspecification of F

Since F is unknown in practice and has to be determined, we now present results on the robustness of our procedure to misspecifications of F . When the p-values are computed from a t-test, the only unknown parameter of F in Eq. (11) is the non-centrality parameter μ_t , which depends on the effect size θ . We have considered low values of the effect size θ , for which the proposed method tends to be more powerful than *GS* when F is correctly specified (see the previous paragraphs). Then we have used different values of the assumed effect size $\hat{\theta}$, so that the true effect sizes is either overestimated ($\theta < \hat{\theta}$) or underestimated ($\theta > \hat{\theta}$). In particular, we have set $\hat{\theta} \in \{\theta - 0.1, \theta - 0.2\}$ for $\theta = 0.8$ and $\theta = 1.2$; additionally, we have used $\hat{\theta} \in \{\theta + 0.1, \theta + 0.2\}$ with $\theta \in \{0.4, 0.6, 0.8, 1\}$. Results are given under independence of the p-values ($\rho = 0$). Note that the performance of the *GS* procedure is not influenced by misspecification of F .

When θ is overestimated, all methods determine valid confidence bounds. Otherwise, confidence bounds determined using any family with $\gamma^* = 1$ are no longer valid. If θ is overestimated, the power of the proposed procedure decreases as the difference between θ and $\hat{\theta}$ increases. For smaller effect sizes ($\theta \leq 0.8$) the proposed procedure with any family and $\gamma^* = 1$ is more powerful than *GS*. If θ is underestimated, the proposed method is more powerful than *GS*, using any family and the largest $\gamma < 1$ for which the method determines valid confidence bounds. Finally, the empirical variance of the proposed method with any critical vector returning valid confidence bounds increases compared to the case of correct specification of F .

5.4 Dependency among the p-values and misspecification of F

In practice, both assumptions of the p-value model can be violated at the same time. In this subsection we therefore show results for dependency of the p-values and misspecification of F . The level of correlation ρ as well as the assumed and true effect sizes, $\hat{\theta}$ and θ , have been fixed as in the previous subsections. When θ is overestimated, all methods determine valid confidence bounds if the effect size is large enough

($\theta \geq 0.8$) or strongly overestimated ($\hat{\theta} \geq \theta + 0.2$). When θ is underestimated, our procedure with any family and low γ^* determines valid confidence bounds for any level of correlation ($\rho > 0$). As in the previous paragraphs, we have considered only critical vectors leading to valid confidence bounds. If θ is overestimated, the proposed method with any family is more powerful than *GS* for small values of θ and all correlations ρ . If θ is underestimated, on the contrary, *GS* is generally more powerful. When the signal is sparse (small m_1) and $\hat{\theta} \leq 0.8$, the empirical variance of *GS* always increases faster than that of the proposed method as ρ increases. This does not necessarily hold true when the signal is dense.

In summary, these simulations emphasize the importance of the choice of the critical vector for the power and robustness of our procedure. Our results imply that the critical vector should not always be chosen to optimize power under the independence assumption. As a rule of thumb, under the normal distribution model, if the effect size is large ($\theta \leq 1$) using $\gamma^* = 1$ should lead to valid confidence bounds, otherwise it is advised to use $\gamma^* < 1$. If the effect size is so small that defining critical vectors such that $\gamma^* < 1$ is impossible, it is sensible to use a constant larger than the predetermined effect size $\hat{\theta}$ to ensure the validity of the bounds. These considerations emphasize the need to find reliable estimates for the effect size.

5.5 Estimating the effect size

The parameters of the CDF F of the p-values under the alternative are generally not known. Then, one possibility is to estimate those parameter values on the basis of similar data. If such additional data are not available, the data set under study can be split into two parts; one part can be used to estimate the parameters, and the other to apply the method. This strategy is similar to Blain et al. (2022), who use an additional data set to construct a family of critical vectors.

In this section we present an approach to estimate F as in Eq. (11) when each p-value P_i is derived from a one-sample two-sided t-test, and thus from a t-statistic Q_i , as in the setting of our simulations. All the t-test statistics and p-values, respectively, are assumed to be independent. The only unknown parameter in the model described at the beginning of this section is the non-centrality parameter μ , as the degrees of freedom $\nu = N - 1$ only depend on the sample size. All other relevant quantities, including the CDF F of the p-values under the alternative, are determined by μ and ν by virtue of Eq. (11).

If we knew which t-statistics correspond to false null hypotheses (e.g., Q_1, \dots, Q_{m_1}), we could use them to easily compute an estimate $\hat{\mu}$ of μ . Indeed,

$$E[Q_i] = \mu \cdot \sqrt{\frac{\nu}{2}} \left(\frac{\Gamma((\nu-1)/2)}{\Gamma(\nu/2)} \right) \quad (i = 1, \dots, m_1)$$

and so

$$\hat{\mu} = \bar{q} \cdot \sqrt{\frac{2}{\nu}} \left(\frac{\Gamma(\nu/2)}{\Gamma((\nu-1)/2)} \right), \quad \bar{q} = \frac{1}{m_1} \sum_{i=1}^{m_1} q_i \quad (12)$$

where q_i is the observed value of Q_i . Then the effect size θ could be immediately estimated with $\hat{\theta} = \hat{\mu} \cdot \sqrt{2/N}$.

In practice, it is unknown which null hypotheses are false. Therefore, we suggest to compute t-statistics for all m coordinates and use a thresholding scheme to decide which coordinates are considered as alternative. A first intuitive strategy is selecting those t-statistics that are not smaller than a given threshold, which may be chosen, for instance, as the empirical ω -quantile of all the t-statistics. A second, similar strategy is selecting the t-statistics for which the corresponding p-value does not exceed a threshold. This threshold may be either a fixed value c or the threshold of a single-step test controlling the FWER, i.e., the probability of selecting at least one t-statistic corresponding to a true null hypothesis. We consider the Bonferroni and Šidák corrections controlling the FWER at level a (see Dickhaus 2014, Section 5). However, other thresholds could be utilized as well. Notice that the threshold increases with a . An algorithm for this second strategy is given in Appendix B.

We have used the previous simulation setting to study the performance of different selection criteria. Based on the results from the previous simulation study, the goal is finding precise estimators while avoiding underestimation of the effect size. We have considered the thresholds for the t-values based on the ω -quantiles with $\omega \in \{25\%, 50\%\}$; then the thresholds for the p-values based on fixed $c \in \{0.01, 0.1\}$ and on FWER control with level $a \in \{0.01, 0.05, 0.1\}$. When no t-values were selected, the effect size has been set to zero. In practice, this would lead to a valid TDP confidence bound equal to zero, as all null hypotheses would be assumed to be true.

Generally, the estimated effect size increases with the denseness of the signal while the empirical variance of all estimators decreases. Using thresholds for the t-values leads to general underestimation of the effect size. Therefore this strategy is not suitable.

The performance of thresholds for the p-values depends on the true effect size θ . For small effect sizes, large threshold values rarely lead to an underestimate. Using small values often leads to an estimated effect size of zero; otherwise, the effect size is generally overestimated. As the true effect size increases, both strategies may underestimate the effect size. This is more severe for large values of the thresholds (i.e., large values of c and a) and in general more frequent when using the fixed thresholds c . When the level of correlation ρ increases, fixed thresholds c lead to less underestimation than FWER-based thresholds.

These simulations support the use of thresholds for the p-values. The value of the threshold should be large when the true effect size θ is small, and small when θ is large. In practice we would therefore recommend to estimate the effect size using FWER-based thresholds with small values of a (e.g. $a \leq 0.01$) if the data are assumed to be normally distributed and a two-sided one-sample t-test is applied. If this leads to an effect size of zero, the threshold can be increased.

6 fMRI study

In this section, we present results obtained from the analysis of a real fMRI data set. The aim of task-related fMRI is to identify regions in the brain that react to a stimulus.

To do so, researchers measure the blood oxygenation level dependent (BOLD) signal in different voxels and at different time points; the experiment is usually repeated for several subjects. Multi-subject data in the context of fMRI are typically analyzed using two-level mixed-effects models (Lindquist 2008). At the first level, data of the individual subjects are analyzed. The output of the first level is used as input of the second level, which is the group analysis. Subjects are then considered as random effects (Poldrack et al. 2011). Suppose that the study considers m voxels, W time points and N subjects. Furthermore, suppose that the stimuli of interest can be coded using L conditions. In a first level analysis, the pre-processed BOLD signal is fitted to a theoretical BOLD signal using a generalized linear model (GLM) :

$$\tilde{Y}_{ij} = X_{ij} \cdot \beta_{ij} + \varepsilon_{ij} \quad (i = 1, \dots, m; j = 1, \dots, N)$$

where $\tilde{Y}_{ij} \in \mathbb{R}^W$ represents the pre-processed time series of the observed BOLD response for the i th voxel and j th subject. The design matrix $X_{ij} \in \mathbb{R}^{W \times K}$ accounts for the theoretical BOLD signal of the L conditions as well as nuisance parameters, such that $K \geq L$. Finally, $\beta_{ij} = (\beta_{ij1}, \dots, \beta_{ijK})^\top$ is the vector of coefficients and $\varepsilon_{i,j} \in \mathbb{R}^W$ is assumed to follow an AR(2)-process (Lindquist 2008).

The beta coefficients are used in the second level analysis to find voxels reacting to the stimulus of interest. They are considered to be random variables. Often, researchers want to find differences in brain activation between two stimuli, a so-called contrast. In this case, for each subject the difference between two stimulus-specific beta coefficients is computed, that is

$$D_{ij} = \beta_{ij1} - \beta_{ij2}, \quad D_{ij} = \mu_i + \xi_{ij},$$

where D_{ij} denotes the contrast of the i th voxel and j th subject and ξ_{ij} is normally distributed with mean zero. These values are then used in the group analysis to test at each voxel i the null hypothesis $H_0 : \mu_i = 0$, using a one-sample two-sided t-test (Lindquist 2008). Therefore, the entire analysis produces a map of t-statistics Q_1, \dots, Q_m and the corresponding map of p-values P_1, \dots, P_m . There are over 100,000 voxels within the brain (Lindquist 2008) and inference on sets of contiguous voxels is of interest. Given a pre-defined region of interest (ROI), that is, a pre-defined set of contiguous voxels, and the p-values for the corresponding voxels, our procedure computes a lower confidence bound for the proportion of active voxels (TDP). The pipeline for the entire analysis is illustrated in Appendix D.

We have considered fMRI studies which investigate the difference between listening to sounds produced by human voice versus non-human sounds. ROIs have been defined based on Schirmer et al. (2012) and Binder et al. (2000). The shape and location of the ROIs have been chosen based on the reported peaks of activation and size of the clusters. In total, we have analyzed six ROIs, two located in the left hemisphere, the left Superior Temporal Gyrus (L STG) and left Auditory Cortex (L AC), and four located in the right hemisphere, the right Auditory Cortex (R AC), the right Fusiform Gyrus (R FG), the right Superior Temporal Gyrus (R STG) and right Middle Temporal Gyrus (R MTG). Further information on the definition and attributes of the ROIs are given in Appendix D.

We have studied fMRI data collected by Pernet et al. (2015) and available at <https://openneuro.org/datasets/ds000158/versions/1.0.0> to compute confidence bounds for the TDP. In this experiment, participants passively listened to a human voice versus non-human sounds. Pre-processed data and contrast maps as results of the first-level analysis for 140 subjects are available at <https://github.com/angeella/fMRIdata/tree/master/data-raw/AuditoryData> and have been used in this study. Further information about pre-processing and first level analysis can be found in Andreella et al. (2023). For each pre-specified ROI, we have applied our methodology as follows. Since the procedure requires knowledge about (the parameters of) F , we have randomly split the subjects in two subgroups to estimate the effect size ($N^{[e]} = 50$) and compute the confidence bounds ($N^{[b]} = 90$). Within each of the two subsets, we have tested the null hypothesis for each voxel in the ROI that there is no difference between the activation caused by human voice vs. non-human sounds and obtained t-value and p-value maps, using the pARI package in R (Andreella 2022).

The effect sizes for the ROIs have been estimated using Eq. (12). As suggested in the simulation study, we have used a p-value threshold based on the Šidák correction with $\alpha = 0.01$. Since this led to an estimated effect size of zero for the ROI “R FG”, we have used the fixed threshold $c = 0.1$ for this ROI. The estimated effect size within each ROI are displayed in table 1.

To compute 80%-confidence bounds for the TDP, we have considered the families introduced in Section 4 and, for each ROI and each family, we have selected a critical vector based on the effect size and suggestions given in Section 5. For ROIs with large effect sizes ($\hat{\theta} \geq 1.2$), we have fixed the critical vectors to optimize Eq. (9), that is $\gamma^* = 1$. For “R AC” we have taken $\gamma^* = 0.95$. Finally, since “R FG” has a very small effect size ($|\hat{\theta}| < 0.4$) we have replaced the effect size by the constant 0.5 and considered $\gamma^* = 1$. Based on the effect size and critical vectors, we have then computed the lower confidence bounds for the TDP.

Table 1 contains the confidence bounds obtained using the proposed procedure with different families, as well as the confidence bounds based on the method by Goeman & Solari (2011). Within each ROI, different choices of the family lead to similar result. Furthermore, these are equivalent to *GS* for ROIs with large (estimated) effect size ($\hat{\theta} > 1$). For the cluster “R AC”, the proposed procedure based on the *Exp* family with $\gamma^* = 0.95$ determines the largest bounds. The proposed method based on the *BH*, *BY* and *AORC* family with $\gamma^* = 0.95$ determine confidence bounds smaller than the *GS* procedure. For the cluster “R FG”, our procedure returns higher bounds than *GS*. This is in accordance with the results of the simulation study, which indicated that our procedure has similar power to *GS* for larger effect sizes and is more powerful than *GS* for smaller effect sizes.

These result suggest that most of the ROIs found by Schirmer et al. (2012) and Binder et al. (2000) are well defined and truly relevant for human voice processing in contrast to non-verbal sound processing. Even though we have explored different ROIs, it has to be noted that the proposed procedure is constructed to study a single, pre-fixed region of interest. Furthermore, the validity of the resulting confidence bounds is based on the assumption that the effect size is not underestimated and

that the choice of γ^* accounts for possible correlations between voxels. This emphasizes the importance of choosing appropriate values for both $\hat{\theta}$ and γ^* .

7 Discussion

We have presented a procedure to compute lower confidence bounds for the TDP for a fixed set of null hypotheses. In contrast to established procedures, our method utilizes a step-up multiple testing procedure and computes the confidence bounds based on the distribution of the respective number of rejections. The proposed method assumes that the p-values corresponding to the null hypotheses of interest are stochastically independent and that the distribution of the p-values under the alternative is known. We have demonstrated through simulations that the proposed procedure is more powerful than the established method of Goeman & Solari (2011) in certain scenarios and, if the settings of the procedure are chosen properly, it can be robust against some violations of the assumptions. Then we have demonstrated how to use the method for fMRI data analysis, when inference is made on a region of interest defined a priori, e.g., to test the reproducibility of a study or to explore if a region associated with a certain task is active when performing another task.

The proposed method is based on a generic choice of the critical vector of a step-up procedure. The observed number of rejections as well as a quantity γ^* , which depends on the distribution of the random number of rejections, are used to compute the confidence bounds. While the procedure defines a valid confidence bound for any choice of the critical vector, the choice influences the power of the proposed procedure. We have given guidelines on how to select an appropriate critical vector from a pre-fixed family indexed by a parameter λ (and in some cases additional parameters). In particular for normally distributed data we have illustrated that in most cases power is maximized for the critical vector having the largest λ such that $\gamma^* = 1$.

If the data are normally distributed and the aforementioned assumptions are met, we have demonstrated through simulation that, for small effect sizes, the proposed procedure can be more powerful than the method of Goeman & Solari (2011). For larger effect sizes, the method by Goeman & Solari (2011) is slightly more powerful but results have higher variability. Furthermore, we have investigated the robustness of the proposed procedure against violations of the assumptions. For large effect sizes, the proposed method is robust to positive dependency among the p-values. If the effect size is small, critical vectors should be chosen such that $\gamma^* < 1$ to obtain valid confidence bounds. The computation of the confidence bounds utilizes information about the effect size, which can be determined using either prior information or estimation based on external information. If the true effect size is overestimated in absolute value, i.e., the true effect size is smaller than the assumed effect size in absolute value, the proposed procedure using any family and $\gamma^* \leq 1$ returns valid confidence bounds. This cannot be ensured if the true effect size is underestimated, again in absolute value. This emphasizes the need for a good estimation procedure for the effect size.

Future work will focus on extending the proposed procedure to account for dependency among the p-values. To do so, the distribution of the number of rejections under dependency of the p-values is needed. Some approaches are given in Roquain & Villers (2011) and would have to be adapted to fit our requirements. Another possible direction for future research consists in obtaining simultaneity of the proposed methods over several (or even all possible) subsets of an original set of null hypotheses. In the fMRI example, this original set of null hypotheses could for instance refer to all measured voxels. Conceptually, this simultaneity can be achieved by applying the closed testing principle and carrying out our proposed method for every intersection null hypothesis in the closure (with respect to intersections) of the original set of null hypotheses. However, proceeding (naively) in this manner will induce a huge computational effort, such that computational shortcuts are desirable. The development of such shortcuts appears challenging and interesting at the same time. Finally, it appears desirable to analyze the choice of the tuning parameters of our procedure also from a theoretical point of view (complementing the numerical evidence from computer simulations), and for more general models than those assuming normally distributed data.

8 Funding acknowledgement

Friederike Preusse gratefully acknowledges funding by the Deutsche Forschungsgemeinschaft (DFG, German Research Foundation)- project number 281474342.

Anna Vesely and Thorsten Dickhaus acknowledge financial support by the Deutsche Forschungsgemeinschaft (DFG) via Grant No. DI 1723/5-3.

9 Data availability

The data used in this article are available at the OpenNeuro dataset ds000158 at <https://openneuro.org/datasets/ds000158/versions/1.0.0> (raw data) and <https://github.com/angeella/fMRIdata/tree/master/data-raw/AuditoryData> (pre-processed data). The code for the simulation and analysis is available upon request from the authors.

References

- Andreella, A. (2022). pari: Permutation-based all-resolutions inference method [Computer software manual]. Retrieved from <https://CRAN.R-project.org/package=pARI> (R package version 1.1.1)
- Andreella, A., Hemerik, J., Finos, L., Weeda, W., & Goeman, J. J. (2023). Permutation-based true discovery proportions for functional magnetic resonance imaging cluster analysis. *Statistics in Medicine*, 42(14), 2311-2340.
- Benjamini, Y., & Hochberg, Y. (1995). Controlling the False Discovery Rate: A Practical and Powerful Approach to Multiple Testing. *Journal of the Royal Statistical Society: Series B (Methodological)*, 57(1), 289-300.
- Benjamini, Y., & Hochberg, Y. (2000). On the Adaptive Control of the False Discovery Rate in Multiple Testing With Independent Statistics. *Journal of Educational and Behavioral Statistics*, 25(1), 60-83.
- Benjamini, Y., & Yekutieli, D. (2001). The control of the false discovery rate in multiple testing under dependency. *The Annals of Statistics*, 29(4), 1165 – 1188.
- Binder, J., Frost, J., Hammeke, T., Bellgowan, P., Springer, J., Kaufman, J., & Posing, E. (2000). Human Temporal Lobe Activation by Speech and Nonspeech Sounds. *Cerebral Cortex*, 10(5), 512-528.
- Blain, A., Thirion, B., & Neuvial, P. (2022). Notip: Non-parametric true discovery proportion control for brain imaging. *NeuroImage*, 260, 119492.
- Blanchard, G., Neuvial, P., & Roquain, E. (2020). Post hoc confidence bounds on false positives using reference families. *The Annals of Statistics*, 48(3), 1281 – 1303.
- Blanchard, G., & Roquain, E. (2008). Two simple sufficient conditions for FDR control. *Electronic Journal of Statistics*, 2, 963 – 992.
- Cai, M., Vesely, A., Chen, X., Li, L., & Goeman, J. J. (2022). NetTDP: permutation-based true discovery proportions for differential co-expression network analysis. *Briefings in Bioinformatics*, 23(6), bbac417.
- Chen, J., Luo, J., Liu, K., & Mehrotra, D. V. (2011). On power and sample size computation for multiple testing procedures. *Computational Statistics & Data Analysis*, 55(1), 110-122.
- Chen, X., Goeman, J. J., Krebs, T. J. P., Meijer, R. J., & Weeda, W. D. (2023). Adaptive cluster thresholding with spatial activation guarantees using all-resolutions inference. arXiv:2206.13587.
- Cohen, A., & Sackrowitz, H. B. (2007). More on the inadmissibility of step-up. *Journal of Multivariate Analysis*, 98(3), 481-492.
- Davenport, S., Thirion, B., & Neuvial, P. (2022). FDP control in multivariate linear models using the bootstrap. arXiv:2208.13724.
- Dickhaus, T. (2014). *Simultaneous statistical inference with applications in the Life Sciences*. Springer Berlin.
- Ebrahimpoor, M., Spitali, P., Hettne, K., Tsonaka, R., & Goeman, J. J. (2020). Simultaneous Enrichment Analysis of all Possible Gene-sets: Unifying Self-Contained and Competitive Methods. *Briefings in Bioinformatics*, 21(4), 1302-1312.
- Efron, B., Tibshirani, R., Storey, J. D., & Tusher, V. (2001). Empirical Bayes Analysis of a Microarray Experiment. *Journal of the American Statistical Association*,

- 96(456), 1151-1160.
- Ferreira, J. A., & Zwinderman, A. H. (2006). On the Benjamini–Hochberg method. *The Annals of Statistics*, 34(4), 1827 – 1849.
- Finner, H., Dickhaus, T., & Roters, M. (2009). On the false discovery rate and an asymptotically optimal rejection curve. *The Annals of Statistics*, 37(2), 596 – 618.
- Finner, H., Gontscharuk, V., & Dickhaus, T. (2012). False Discovery Rate Control of Step-Up-Down Tests with Special Emphasis on the Asymptotically Optimal Rejection Curve. *Scandinavian Journal of Statistics*, 39(2), 382-397.
- Finner, H., & Roters, M. (2002). Multiple hypotheses testing and expected number of type I errors. *The Annals of Statistics*, 30(1), 220 – 238.
- Genovese, C. R., & Wasserman, L. (2006). Exceedance Control of the False Discovery Proportion. *Journal of the American Statistical Association*, 101(476), 1408-1417.
- Goeman, J. J., Górecki, P., Monajemi, R., Chen, X., Nichols, T. E., & Weeda, W. (2023). Cluster extent inference revisited: quantification and localisation of brain activity. *Journal of the Royal Statistical Society Series B: Statistical Methodology*, 85(4), 1128-1153.
- Goeman, J. J., Hemerik, J., & Solari, A. (2021). Only closed testing procedures are admissible for controlling false discovery proportions. *The Annals of Statistics*, 49(2), 1218 – 1238.
- Goeman, J. J., Meijer, R., & Krebs, T. (2021). hommel: Methods for closed testing with simes inequality, in particular hommel’s method [Computer software manual]. Retrieved from <https://CRAN.R-project.org/package=hommel> (R package version 1.6)
- Goeman, J. J., & Solari, A. (2011). Multiple Testing for Exploratory Research. *Statistical Science*, 26(4), 584 – 597.
- Gontscharuk, V. (2010). *Asymptotic and exact results on FWER and FDR in multiple hypotheses testing* (Doctoral dissertation). Retrieved from <https://d-nb.info/1011975238/34>
- Habiger, J. D., & Adekpedjou, A. (2014). Optimal rejection curves for exact false discovery rate control. *Statistics & Probability Letters*, 94, 21-28.
- Hemerik, J., Solari, A., & Goeman, J. J. (2019). Permutation-based simultaneous confidence bounds for the false discovery proportion. *Biometrika*, 106(3), 635-649.
- Hwang, Y.-T. (2011). Comparisons of estimators of the number of true null hypotheses and adaptive FDR procedures in multiplicity testing. *Journal of Statistical Computation and Simulation*, 81(2), 207-220.
- Jenkinson, M., Beckmann, C. F., Behrens, T. E., Woolrich, M. W., & Smith, S. M. (2012). FSL. *NeuroImage*, 62(2), 782-790.
- Katsevich, E., & Ramdas, A. (2020). Simultaneous high-probability bounds on the false discovery proportion in structured, regression and online settings. *The Annals of Statistics*, 48(6), 3465 – 3487.
- Laird, A. R., Robinson, J. L., McMillan, K. M., Tordesillas-Gutiérrez, D., Moran, S. T., Gonzales, S. M., . . . Lancaster, J. L. (2010). Comparison of the disparity between Talairach and MNI coordinates in functional neuroimaging data: Valid-

- tion of the Lancaster transform. *NeuroImage*, 51(2), 677-683.
- Lancaster, J. L., Tordesillas-Gutiérrez, D., Martinez, M., Salinas, F., Evans, A., Zilles, K., ... Fox, P. T. (2007). Bias between MNI and Talairach coordinates analyzed using the ICBM-152 brain template. *Human Brain Mapping*, 28(11), 1194-1205.
- Lancaster, J. L., Woldorff, M. G., Parsons, L. M., Liotti, M., Freitas, C. S., Rainey, L., ... Fox, P. T. (2000). Automated Talairach Atlas labels for functional brain mapping. *Human Brain Mapping*, 10(3), 120-131.
- Lee, W., Gusnanto, A., Salim, A., Magnusson, P., Sim, X., Tai, E., & Pawitan, Y. (2012). Estimating the number of true discoveries in genome-wide association studies. *Statistics in Medicine*, 31(11-12), 1177-1189.
- Lindquist, M. A. (2008). The Statistical Analysis of fMRI Data. *Statistical Science*, 23(4), 439 – 464.
- Marcus, R., Eric, P., & Gabriel, K. R. (1976). On closed testing procedures with special reference to ordered analysis of variance. *Biometrika*, 63(3), 655-660.
- Meinshausen, N. (2006). False Discovery Control for Multiple Tests of Association Under General Dependence. *Scandinavian Journal of Statistics*, 33(2), 227-237.
- Patra, R. K., & Sen, B. (2016). Estimation of a Two-component Mixture Model with Applications to Multiple Testing. *Journal of the Royal Statistical Society Series B: Statistical Methodology*, 78(4), 869-893.
- Pernet, C. R., McAleer, P., Latinus, M., Gorgolewski, K. J., Charest, I., Bestelmeyer, P. E., ... Belin, P. (2015). The human voice areas: Spatial organization and inter-individual variability in temporal and extra-temporal cortices. *NeuroImage*, 119, 164-174.
- Poldrack, R. A., Mumford, J. A., & Nichols, T. E. (2011). *Handbook of Functional MRI Data Analysis*. Cambridge University Press.
- R Core Team. (2022). R: A language and environment for statistical computing [Computer software manual]. Vienna, Austria. Retrieved from <https://www.R-project.org/>
- Roquain, E., & Villers, F. (2011). Exact calculations for false discovery proportion with application to least favorable configurations. *The Annals of Statistics*, 39(1), 584 – 612.
- Rosenblatt, J. D., Finos, L., Weeda, W. D., Solari, A., & Goeman, J. J. (2018). All-Resolutions Inference for brain imaging. *NeuroImage*, 181, 786-796.
- Sarkar, S. K. (2002). Some Results on False Discovery Rate in Stepwise multiple testing procedures. *The Annals of Statistics*, 30(1), 239 – 257.
- Schirmer, A., Fox, P. M., & Grandjean, D. (2012). On the spatial organization of sound processing in the human temporal lobe: A meta-analysis. *NeuroImage*, 63(1), 137-147.
- Simes, R. J. (1986). An improved Bonferroni procedure for multiple tests of significance. *Biometrika*, 73(3), 751-754.
- Storey, J. D., Taylor, J. E., & Siegmund, D. (2004). Strong control, conservative point estimation and simultaneous conservative consistency of false discovery rates: a unified approach. *Journal of the Royal Statistical Society: Series B (Statistical Methodology)*, 66(1), 187-205.
- Tian, J., Chen, X., Katsevich, E., Goeman, J. J., & Ramdas, A. (2023). Large-scale simultaneous inference under dependence. *Scandinavian Journal of Statist-*

- ics*, 50(2), 750-796.
- Vesely, A., Finos, L., & Goeman, J. J. (2023). Permutation-based true discovery guarantee by sum tests. *Journal of the Royal Statistical Society Series B: Statistical Methodology*, 85(3), 664-683.
- von Schroeder, J. (2018). Ordstat: Calculate the joint distribution of order statistics [Computer software manual]. (R package version 1.0)
- von Schroeder, J., & Dickhaus, T. (2020). Efficient calculation of the joint distribution of order statistics. *Computational Statistics & Data Analysis*, 144, 106899.

10 Tables

Table 1 fMRI data: analysis of different ROIs. Number of voxels m , estimated effect size $\hat{\theta}$ and lower confidence bound $\hat{\pi}_1$ for the TDP obtained from the method of Goeman & Solari (2011) (GS) and the proposed procedure with different families of critical vectors (BH_{γ^*} , BY_{γ^*} , $AORC_{\gamma^*}$, Exp_{γ^*}). The value γ^* was chosen based on the suggestions given in Section 5.

ROI	Size lvoxell	Effect size	$\hat{\pi}_1$ computed using:				
			GS	BH_{γ^*}	BY_{γ^*}	$AORC_{\gamma^*}$	Exp_{γ^*}
L STG	162	1.3222	1	1	1	1	1
L AC	33	1.4440	1	1	1	1	1
R AC	257	0.9400	0.4825	0.4397	0.4397	0.4591	0.5175
R FG	81	-0.3444	0.1605	0.2222	0.2222	0.2222	0.2222
R MTG	257	1.5204	1	1	1	1	1
R STG	389	1.6570	1	1	1	1	1

11 Figures

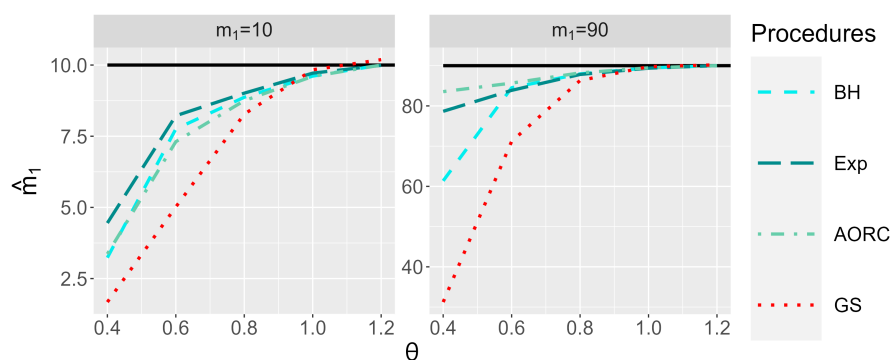


Figure 1 Independence setting: p-values have correlation $\rho = 0$ and the effect size θ is known. Lower confidence bound \hat{m}_1 for the number of true discoveries m_1 obtained from the proposed procedure with different families of critical vectors (BH_{opt} , Exp_{opt} , $AORC_{opt}$) and the method of Goeman & Solari (2011) (GS). The black solid line corresponds to m_1 .

A Proofs

Theorem 1

The number of true discoveries m_1 is an unknown integer between 0 and m . Fix a candidate value $\tilde{m}_1 \in \{0, \dots, m\}$, as well as the probability $\mathbb{P}_{\tilde{m}_1}$ under the corresponding model. From Eq. (2), the value $\gamma_{\tilde{m}_1}$ is such that

$$\mathbb{P}_{\tilde{m}_1}(\tilde{m}_1 \geq R\gamma_{\tilde{m}_1}) \geq 1 - \alpha.$$

Then consider the minimum γ^* of these values, as defined in Eq. (3). For any \tilde{m}_1 , we have that $R\gamma^* \leq R\gamma_{\tilde{m}_1}$, and so

$$\mathbb{P}_{\tilde{m}_1}(\tilde{m}_1 \geq R\gamma^*) \geq \mathbb{P}_{\tilde{m}_1}(\tilde{m}_1 \geq R\gamma_{\tilde{m}_1}) \geq 1 - \alpha.$$

This holds in particular for the true value m_1 , so that

$$\mathbb{P}_{m_1}(m_1 \geq R\gamma^*) \geq 1 - \alpha.$$

Finally, recall that m_1 can take only integer values. Hence

$$m_1 \geq R\gamma^* \iff m_1 \in \{\lceil R\gamma^* \rceil, \dots, m\} \iff m_1 \geq \lceil R\gamma^* \rceil$$

and so

$$\mathbb{P}_{m_1}(m_1 \geq \lceil R\gamma^* \rceil) = \mathbb{P}_{m_1}(m_1 \geq R\gamma^*) \geq 1 - \alpha.$$

Therefore $\hat{m}_1 = \lceil R\gamma^* \rceil$ is a lower $(1 - \alpha)$ -confidence bound for m_1 .

Theorem 2

From Eq. (2)

$$\gamma_{\tilde{m}_1} = \max \{ \gamma \in [0, 1] : \mathbb{P}_{\tilde{m}_1}(R\gamma \leq \tilde{m}_1) \geq 1 - \alpha \}.$$

Recall that R is a discrete variable taking values in $\{0, \dots, m\}$, so it is sufficient to study its CDF in these values. First, suppose that $\tilde{m}_1 = 0$. In this case,

$$\mathbb{P}_0(R\gamma \leq 0) = \mathbb{P}_0(R\gamma = 0) = \begin{cases} 1 & \text{if } \gamma = 0 \\ \mathbb{P}_0(R = 0) & \text{if } \gamma \in (0, 1]. \end{cases}$$

Hence it is sufficient to look for the maximum in $\{0, 1\}$:

$$\gamma_0 = \max \{ \gamma \in \{0, 1\} : \mathbb{P}_0(R\gamma = 0) \geq 1 - \alpha \} = \begin{cases} 1 & \text{if } \mathbb{P}_0(R = 0) \geq 1 - \alpha \\ 0 & \text{otherwise} \end{cases}$$

Then consider any other value $\tilde{m}_1 \in \{1, \dots, m\}$. Notice that for $\gamma = \tilde{m}_1/m$ we obtain

$$\mathbb{P}_{\tilde{m}_1}(R\gamma \leq \tilde{m}_1) = \mathbb{P}_{\tilde{m}_1}(R \leq m) = 1 \geq 1 - \alpha,$$

and so $\gamma_{\tilde{m}_1} \geq \tilde{m}_1/m > 0$. Then we can re-write

$$\begin{aligned} \gamma_{\tilde{m}_1} &= \max \left\{ \gamma \in \left[\frac{\tilde{m}_1}{m}, 1 \right] : \mathbb{P}_{\tilde{m}_1} \left(R \leq \frac{\tilde{m}_1}{\gamma} \right) \geq 1 - \alpha \right\} \\ &= \max \left\{ \gamma \in \left\{ \frac{\tilde{m}_1}{m}, \frac{\tilde{m}_1}{m-1}, \dots, \frac{\tilde{m}_1}{\tilde{m}_1} \right\} : \mathbb{P}_{\tilde{m}_1} \left(R \leq \frac{\tilde{m}_1}{\gamma} \right) \geq 1 - \alpha \right\} \\ &= \max \left\{ \gamma = \frac{\tilde{m}_1}{\ell}, \ell \in \{\tilde{m}_1, \dots, m-1, m\} : \mathbb{P}_{\tilde{m}_1}(R \leq \ell) \geq 1 - \alpha \right\} \\ &= \frac{\tilde{m}_1}{\ell_{\tilde{m}_1}} \end{aligned}$$

where

$$\ell_{\tilde{m}_1} = \min \{ \ell \in \{\tilde{m}_1, \dots, m-1, m\} : \mathbb{P}_{\tilde{m}_1}(R \leq \ell) \geq 1 - \alpha \}.$$

From this, it follow that

$$\gamma_{\tilde{m}_1} = \tilde{m}_1 / \ell_{\tilde{m}_1}.$$

Proposition 1

Denote by $S = |\mathcal{R} \cap \mathcal{M}_1|$ the random variable corresponding to the number of true discoveries in the rejection set \mathcal{R} , and by $V = R - S$ the random variable corresponding to the number of false discoveries. We use that $R = V + S$, then by the law of total probability

$$\begin{aligned} \mathbb{P}_{\tilde{m}_1}(R = \ell) &= \sum_{j=0}^{\ell} \mathbb{P}_{\tilde{m}_1}(V = j, S = \ell - j) \\ &= \sum_{j=0}^{\ell} \binom{m - \tilde{m}_1}{j} \binom{\tilde{m}_1}{\ell - j} t_{\ell}^j (F(t_{\ell}))^{\ell - j} \\ &\quad \cdot \Psi_{m - \tilde{m}_1 - j, \tilde{m}_1 - \ell + j}^{Uni[0,1], \bar{F}}(1 - t_m, \dots, 1 - t_{\ell+1}), \end{aligned}$$

The last equality is due to Roquain & Villers (2011), Section 5.3. The expression for $\mathbb{P}_{\tilde{m}_1}(R = \ell)$ given in the proposition follows.

Proposition 2

Because R is discrete, $\mathbb{P}_{\tilde{m}_1}(R = \ell) = \mathbb{P}_{\tilde{m}_1}(R \leq \ell) - \mathbb{P}_{\tilde{m}_1}(R \leq \ell - 1)$. Thus, the expected value of R can be computed as

$$E_{\tilde{m}_1}[R] = \sum_{\ell=0}^m \ell \cdot \mathbb{P}_{\tilde{m}_1}(R = \ell) = \sum_{\ell=0}^m \ell \cdot (\mathbb{P}_{\tilde{m}_1}(R \leq \ell) - \mathbb{P}_{\tilde{m}_1}(R \leq \ell - 1)),$$

where $\mathbb{P}_{\tilde{m}_1}(R \leq \ell)$ is given in Proposition 1. The expression of $E_{\tilde{m}_1}[R\gamma^k]$ follows.

Similarly, the variance is computed as

$$\begin{aligned} \text{Var}_{\tilde{m}_1}[R] &= E_{\tilde{m}_1}[R^2] - E_{\tilde{m}_1}[R]^2 \\ &= \sum_{\ell=0}^m \ell^2 \cdot (\mathbb{P}_{\tilde{m}_1}(R \leq \ell) - \mathbb{P}_{\tilde{m}_1}(R \leq \ell - 1)) - \left(\sum_{\ell=0}^m \ell \cdot (\mathbb{P}_{\tilde{m}_1}(R \leq \ell) - \mathbb{P}_{\tilde{m}_1}(R \leq \ell - 1)) \right)^2. \end{aligned}$$

B Algorithms

In this section, we give algorithms for the proposed methodology.

Algorithm 1 computes a lower $(1 - \alpha)$ -confidence bound \hat{m}_1 for the number of true discoveries as in Eq. (4), using results from Theorems 1 and 2 and Proposition 1. Note that observations in form of r are only used in the last step of the algorithm.

Algorithm 2 implements the methods based on thresholds for the p-values to compute an estimate $\hat{\theta}$ of the effect size, as described in Section 5.5. The algorithm uses t-values $\mathbf{q} = (q_1, \dots, q_m)^\top$ and p-values $p = (p_1, \dots, p_m)^\top$. It selects the t-values for which the corresponding p-values do not exceed a given threshold h , and uses those to determine $\hat{\theta}$. The threshold h may be either a fixed value or the threshold based on of a single-step test controlling the FWER at level α , such as the Bonferroni and Šidák corrections. For the Bonferroni correction,

$$h = \frac{\alpha}{m},$$

while for the Šidák correction,

$$h = 1 - (1 - \alpha)^{\frac{1}{m}}.$$

Algorithm 1: Algorithm to compute \hat{m}_1 such that $\mathbb{P}_{m_1}(m_1 \geq \hat{m}_1) \geq 1 - \alpha$ as in Eq. (4).

```

for  $\tilde{m}_1 = 0, \dots, m$  do
   $\ell = -1$ ;
   $Pr = 0$ ;
  while  $Pr < 1 - \alpha$  &  $\ell < m$  do
     $\ell = \ell + 1$ ;
     $Pr = Pr + P(R = \ell)$ ;
  end
  if  $\ell < \tilde{m}_1$  then
     $\ell_{\tilde{m}_1} = \tilde{m}_1$ ;
  else
     $\ell_{\tilde{m}_1} = r$ 
  end
  if  $\ell_{\tilde{m}_1} = 0$  then
     $\gamma_{\tilde{m}_1} = 1$ ;
  else
     $\gamma_{\tilde{m}_1} = \frac{\tilde{m}_1}{\ell_{\tilde{m}_1}}$ 
  end
end
 $\gamma^* = \min_{\tilde{m}_1 \in [m]} (\gamma_{\tilde{m}_1})$ ;
return  $\lceil r \cdot \gamma^* \rceil$ ;

```

Algorithm 2: Algorithm to compute $\hat{\theta}$ based on Eq. (12), using a threshold h for the p-values.

```

 $v = N - 1$ ;
 $\mathbf{q}_{\text{sel}} = \mathbf{q}[\mathbf{p} \leq h]$ ;
 $\hat{\mu} = \text{mean}(\mathbf{q}_{\text{sel}}) \cdot \sqrt{\frac{2}{v} \frac{\Gamma(v/2)}{\Gamma((v-1)/2)}}$ ;
return  $\hat{\mu} \cdot \sqrt{\frac{2}{N}}$ 

```

C Additional simulation results

In this section, further details about the simulations of Section 5 are given. We claim that, for any family of critical vectors indexed by a parameter λ (and eventually other parameters), optimal power is achieved when selecting the largest λ for which $\gamma^* = 1$ in Eq. (3), as mentioned in Section 4. Subsequently, we present additional plots that support the claims on results made in Section 5. Tables and plots are shown only for some choices of the parameters, but other values lead to the same conclusions.

First, consider the setting under Assumption 1, where p-values are independent and the CDF F is correctly specified. Table 2 displays the sum of the expected values given in Eq. (9), obtained using different critical vectors and for varying effect sizes θ . Eq. (9) is maximized when λ is chosen as the largest value for which $\gamma^* = 1$. Furthermore, Table 3 displays the average confidence bounds of the proposed procedure with different critical vectors for a fixed $\theta = 0.8$ and varying values of m_1 . In most cases, the largest confidence bound is obtained for critical vectors with $\gamma^* = 1$, with the only exception of settings with very sparse signal ($m_1 \leq 10$). This justifies the choice of maximizing Eq. (9) to select the critical vector, as in most cases the same critical vector leads to the largest confidence bound.

Figures 2-4 display, for different simulation scenarios, the average lower confidence bounds \hat{m}_1 obtained from GS and the proposed method with different families of critical vectors. Critical vectors of each family have been chosen using the largest $\gamma^* \in \{0.8, 0.9, 0.95, 1\}$ such that the proposed method determines valid confidence bounds. Results are shown for smaller effect sizes ($\theta \leq 1.2$) and the extreme values of the denseness of the signal ($m_1 \in \{10, 90\}$).

In particular, Figure 2 displays results under dependency of the p-values ($\rho = 0.3$) and correct specification of F . Results both for $\gamma^* = 0.8$ and $\gamma^* = 0.95$ are shown, as the first corresponds to valid confidence bounds for very small effect sizes ($\theta \geq 0.6$), while the latter corresponds to valid confidence bounds for slightly larger effect sizes ($\theta \geq 0.8$).

Results under misspecification of F ($\hat{\theta} = \theta + 0.1$) and independence of the p-values are displayed in Figure 3. Critical vectors were chosen using $\gamma^* = 1$.

Lastly, results under dependency of the p-values ($\rho = 0.3$) and misspecification of F ($\hat{\theta} = \theta + 0.1$) are displayed in Figure 4. Critical vectors were chosen using $\gamma^* = 1$.

Additionally, we have considered the setting with dependent p-values and correct specification of F and we have studied the validity of the confidence bounds \hat{m}_1 obtained using any family with $\gamma^* = 1$. Figure 5 illustrates the proportion of iterations for which the lower confidence bound is larger than the true number of discoveries ($m_1 < \hat{m}_1$). If this proportion is larger than α , the bounds are considered to be not valid. Again, results are shown for smaller effect sizes ($\theta \leq 1.2$).

Table 2 Independence setting: p-values have correlation $\rho = 0$ and the effect size θ is known. Sum of the expected values $\mathbb{E}_{\hat{m}_1}[R\gamma^*]$ over all possible candidate values $\hat{m}_1 \in \{0, \dots, m\}$, as given in Eq. (9). Results are obtained from the proposed procedure with different families of critical vectors (BH_{γ^*} , Exp_{γ^*} , $AORC_{\gamma^*}$). Bold values correspond to the highest value of the sum for each θ .

Critical vector	θ				
	0.6	0.8	1	1.2	2
BH_{opt}	4720.33	4910.98	5011.96	5058.00	5065.01
$BH_{0.95}$	4535.58	4702.08	4786.21	4817.20	4820.65
$BH_{0.9}$	4372.23	4504.50	4569.98	4582.53	4584.15
$BH_{0.8}$	3928.18	4079.47	4113.83	4110.73	4106.56
BY_{opt}	4720.44	4911.31	5011.99	5057.98	5065.04
$BY_{0.95}$	4540.14	4700.22	4786.94	4817.05	4820.16
$BY_{0.9}$	4365.37	4505.53	4567.08	4583.50	4583.98
$BY_{0.8}$	3921.54	4065.40	4111.10	4106.36	4111.25
Exp_{opt}	4703.07	4909.88	5012.18	5057.61	5057.37
$Exp_{0.95}$	4548.57	4686.55	4783.07	4818.85	4878.56
$Exp_{0.9}$	4384.82	4481.32	4556.33	4589.78	4724.74
$Exp_{0.8}$	3939.10	4030.66	4084.48	4119.19	4349.03
$AORC_{opt}$	4740.10	4915.25	5012.17	5058.00	5065.06
$AORC_{0.95}$	4604.67	4718.93	4786.76	4815.32	4820.62
$AORC_{0.9}$	4455.21	4531.71	4388.23	4584.36	4586.82
$AORC_{0.8}$	4011.63	4080.76	4101.44	4105.72	4106.77

Table 3 Independence setting: p-values have correlation $\rho = 0$ and the effect size $\theta = 0.8$ is known. Lower confidence bound \hat{m}_1 for the number of true discoveries m_1 obtained from the proposed procedure with different families of critical vectors (BH_{γ^*} , Exp_{γ^*} , $AORC_{\gamma^*}$) and the method of Goeman & Solari (2011) (GS). Bold values correspond to the highest value of \hat{m}_1 for each m_1 .

m_1	10	20	30	40	50	60	70	80	90
GS	8.28	16.87	25.78	35.08	44.66	54.46	64.67	75.15	86.31
BH_{opt}	8.87	18.80	28.78	38.85	48.85	58.72	68.60	78.30	87.95
BY_{opt}	8.87	18.80	28.79	38.85	48.85	58.72	68.60	78.30	87.95
Exp_{opt}	9.01	18.92	28.86	38.88	48.83	58.66	68.50	78.18	87.82
$AORC_{opt}$	8.75	18.66	28.66	38.78	48.86	58.80	68.75	78.52	88.21
$BH_{0.95}$	9.07	18.70	28.19	37.83	47.34	56.76	66.06	75.40	84.35
$BY_{0.95}$	9.06	18.69	28.17	37.81	47.31	56.74	66.04	75.38	84.33
$Exp_{0.95}$	9.13	18.69	28.10	37.70	47.12	56.55	65.78	75.16	84.07
$AORC_{0.95}$	9.03	18.69	28.22	37.91	47.52	56.96	66.38	75.68	84.71

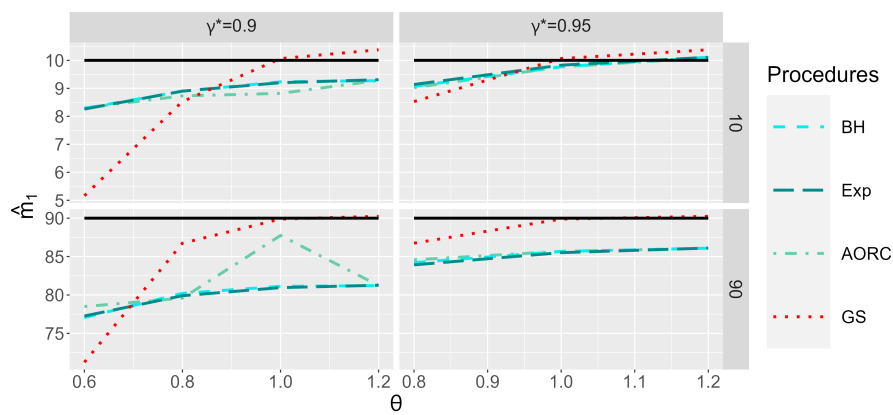


Figure 2 Dependency: p-values have correlation $\rho = 0.3$ and effect size θ is known. Lower confidence bound \hat{m}_1 obtained from the proposed procedure with different critical vectors ($BH_{\gamma^*}, Exp_{\gamma^*}, AORC_{\gamma^*}$) and the method of Goeman & Solari (2011) (GS). The black solid line corresponds to m_1 .

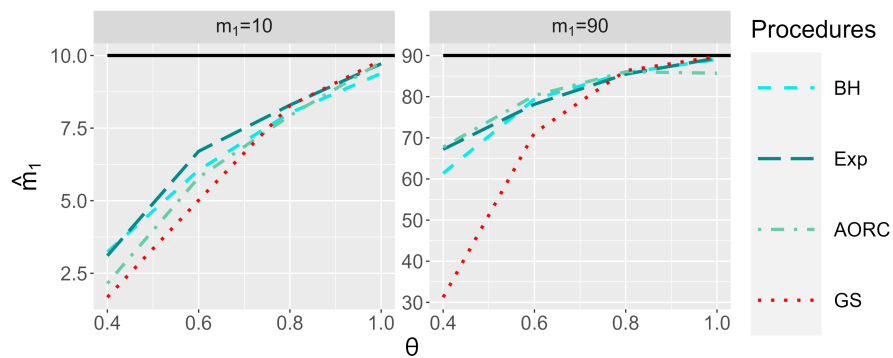


Figure 3 Misspecification of F : p-values have correlation $\rho = 0$ and the true effect size is overestimated ($\hat{\theta} = \theta + 0.1$). Lower confidence bound \hat{m}_1 for the number of true discoveries m_1 obtained from the proposed procedure with different critical vectors ($BH_{opt}, Exp_{opt}, AORC_{opt}$) and the method of Goeman & Solari (2011) (GS). The black solid line corresponds to m_1 .

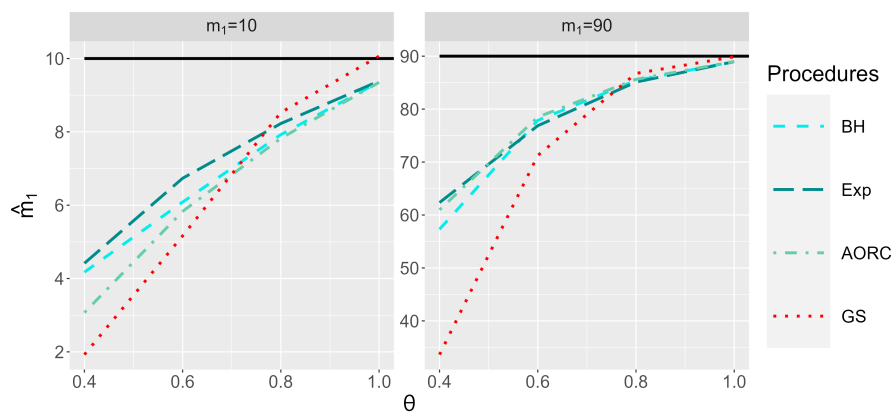


Figure 4 Dependency and misspecification of F : p-values have correlation $\rho = 0.3$ and the true effect size is overestimated ($\hat{\theta} = \theta + 0.1$). Lower confidence bound \hat{m}_1 for the number of true discoveries m_1 obtained from the proposed procedure with different critical vectors (BH_{opt} , Exp_{opt} , $AORC_{opt}$) and the method of Goeman & Solari (2011) (GS). The black solid line corresponds to m_1 .

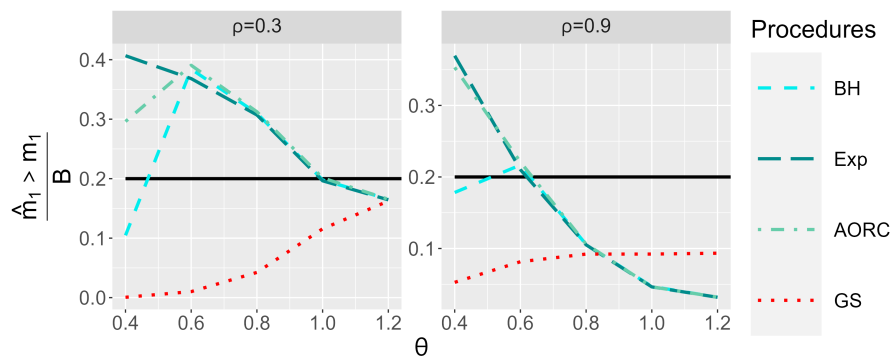


Figure 5 Dependency setting: p-values have correlation ρ and effect size θ is known. Proportion of iterations for which $\hat{m}_1 > m_1$, where \hat{m}_1 is the lower confidence bound for the number of true discoveries $m_1 = 50$ obtained from the proposed procedure with different critical vectors (BH_{opt} , Exp_{opt} , $AORC_{opt}$) and the method of Goeman & Solari (2011). The total number of iterations is $B = 10,000$. The black solid line corresponds to the significance level $\alpha = 0.2$.

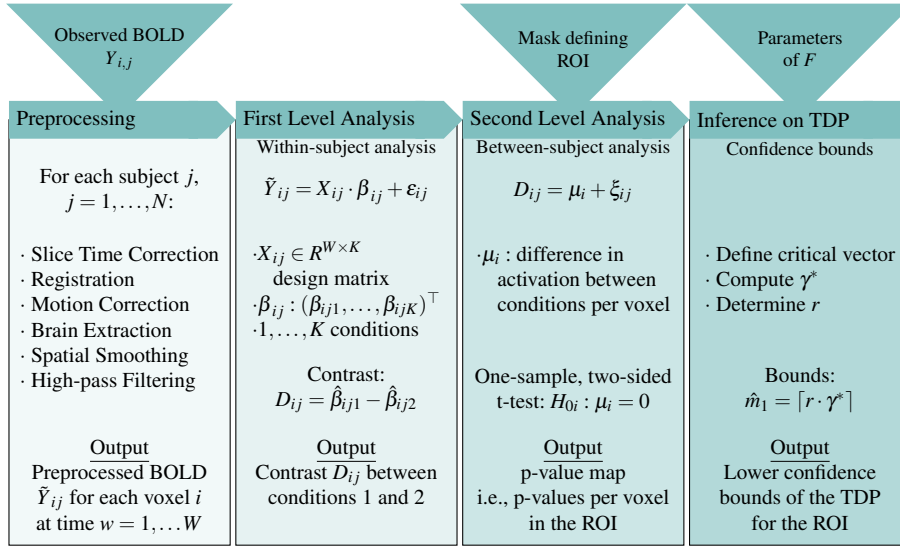


Figure 6 The general steps needed to compute a lower $(1 - \alpha)$ -confidence bound for the TDP within a given ROI. The inputs are, for each voxel and each subject, the measured BOLD time series Y_{ij} and the design matrix X_{ij} .

D Analysis of fMRI data

This section provides additional information on the analysis of fMRI data illustrated in Section 6. First, we describe in greater detail the workflow of the analysis. Then we describe how the ROIs for the considered data set have been defined.

Pipeline for the analysis

The general process of the proposed fMRI analysis is illustrated in Figure 6. The goal of the analysis is computing a lower $(1 - \alpha)$ -confidence bound for the proportion of active voxels (TDP) within a pre-specified ROI. The analysis uses the measured bold time series Y_{ij} and the design matrix X_{ij} for each voxel i and each subject j . The distribution F under the alternative of the p-values obtained from the second level analysis is assumed to be known, i.e., the parameters that characterize F are assumed to be determined prior to the analysis.

Figure 7 further illustrates the last part of the process, where the contrasts obtained from the first level analysis are used to compute the TDP confidence bound. The $N = 140$ subjects are split into two sub-groups; the first is used to estimate the effect size θ , and the second to compute the confidence bound.

Definition of the ROI

ROIs have been defined using the clusters and peaks of activation reported by Schirmer et al. (2012) and Binder et al. (2000), that investigated human voices vs. non-human sounds. In Schirmer et al. (2012), we have considered only the four clusters containing at least 20 voxels with a total of seven peaks of activation. Additionally, we considered two clusters determined by Binder et al. (2000) with a total of eleven peaks of activation. Then we have defined the ROIs from the selected clusters, as following.

ROIs have been defined as either spheres or cuboids. Spherical ROIs have been defined such that they include all peaks of activation in the cluster and have a similar size in mm^3 as the clusters reported in the

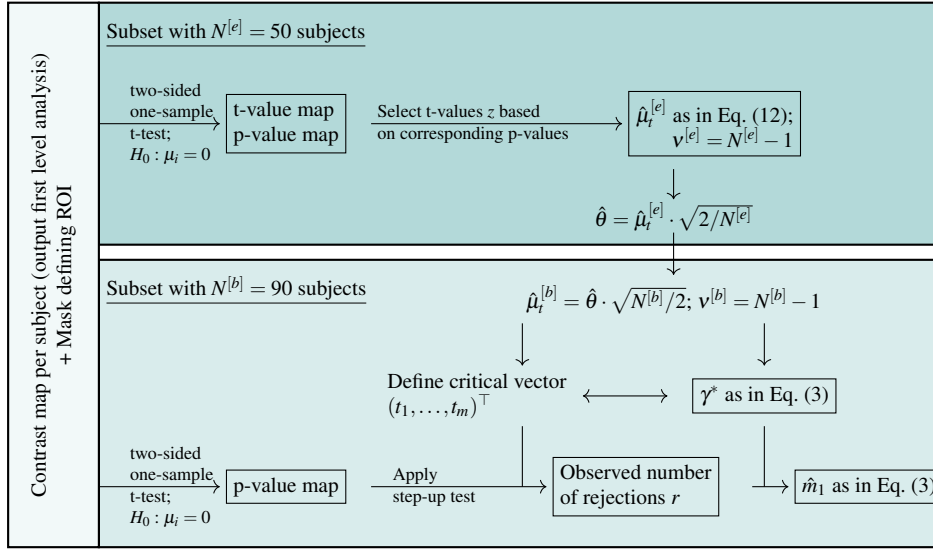


Figure 7 Illustration of the work flow to compute a lower $(1 - \alpha)$ -confidence bound for the TDP within a given ROI. The sample is split into two sub-samples to estimate the effect size and compute the lower confidence bounds separately. For each sub-sample, the inputs are the contrasts $D_{ij} = \mu_i + \xi_{ij}$ of each voxel i and subject j .

corresponding study. Note that only Schirmer et al. (2012) determined the size in mm^3 of the clusters. If the cluster contained more than one peak of activation, the center of the sphere has been defined as the mean voxel coordinate; if the cluster contained only one peak of activation the spherical ROI has been centered around it. If the spherical cluster had a voxel size that differed too much from the one given in Schirmer et al. (2012), a cuboid ROI has been defined, such that each peak of activation was the center of a cube and these cubes were connected. The size of the cubes has been defined such that the resulting size of the ROI was similar to the cluster size given in Schirmer et al. (2012). An overview of the different clusters, including their size and location, is given in Table 4 and illustrated in Figure 8.

We have used the "icbm2tal" transformation in GingerAle (Laird et al. (2010), Lancaster et al. (2007), see also <https://www.brainmap.org/icbm2tal/>) to transform the Talairach coordinates given in Schirmer et al. (2012) to MNI coordinates. We have used FSL (Jenkinson et al. 2012) to create the masks for the ROIs.

Table 4 Information about the regions of interest. The clusters are named according to the area of the brain in which the peak of activation is located, based on the Talairach Daemon Labels in FSL (Lancaster et al. 2000). Given is the shape of the ROI, the width (for cuboid) or radius (for spheres) of the ROIs, the number of peaks of activation and the size of the ROI in terms of number of voxels. Furthermore, for spherical ROI the voxel coordinates [x,y,z] of the center of each sphere are reported, for the cuboid ROI the coordinates of the peaks of activation are reported. The coordinates are given in the MNI152 space.

Reference	ROI	Shape	Radius/width in mm	Size	Peaks	Coordinates		
						x	y	z
Schirmer et al. (2012)	L STG	Cuboid	6	162	3	-38	-38	10
						-44	-30	8
						-50	-20	2
	L AC	Sphere	4	33	2	-60	-18	12
R AC	Sphere	8	257	1	52	-26	18	
Binder et al. (2000)	R FG	Sphere	5	81	1	39	-39	-14
	R MTG	Sphere	8	257	6	64	-4	-8
	R STG	Sphere	9	389	5	58	-30	2

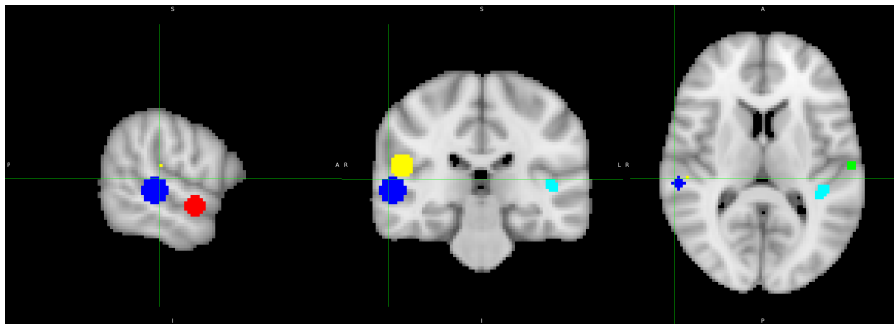


Figure 8 Location of the ROI in the brain. The turquoise region corresponds to the ROI in the Left STG, the green sphere corresponds to the ROI centered in the Left AC, the yellow sphere corresponds to the ROI centered in the Right AC, the blue sphere corresponds to the ROI centered in the Right MTG and the red sphere corresponds to the ROI centered in the Right STG. Note that in the picture on the left the right hemisphere of the brain is shown.